CSMA 2026
17ème Colloque National en Calcul des Structures
18-22 Mai 2026, Presqu'île de Giens (Var)

Enhanced experimental–numerical correlation for the investigation of dynamic instabilities under uncertain frictional interface modeling

S. DURAIN[1,2], J.F. BRUNEL[1], C. HUBERT[3], F. MASSA[2], P. DUFRENOY[1]

[1] *Univ Lille, CNRS, Centrale Lille, UMR 9013 - LaMcube, F-59000, Lille, France*
[2] *Université Polytechnique Hauts-de-France, CNRS, UMR 8201 - LAMIH, 59313 Valenciennes, France*
[3] *INSA Hauts-de-France, Valenciennes, France*

Abstract —This paper presents an enhanced numerical–experimental framework for investigating the dynamic instabilities of a pin–disk system, explicitly accounting for uncertainties at the frictional interface. The main objective is to identify the key parameters that promote the onset of brake squeal on simplified pin on disk system. On the numerical side, the approach combines the quantification and modelling of geometric and material uncertainties, the construction of a modal database via clustering-based modal tracking, and the propagation of uncertainties using data-driven metamodeling. Finally, a multiparametric analysis of the evolution of the contact parameters is performed to characterise mode coupling mechanisms.
Keywords — Experimental–numerical correlation, Dynamic instabilities

1 Introduction

The primary function of automotive braking systems is to ensure user safety. However, brake squeal has emerged over the past decades as a major challenge for automotive manufacturers. Although often perceived by end users as a sign of malfunction, this acoustic phenomenon severely degrades the vibro-acoustic quality and perceived comfort of vehicles. With sound pressure levels that can reach up to 110 dB, squeal represents a particularly complex technical issue.

Predicting the squeal propensity of a brake system is notoriously difficult because squeal is an intrinsically nonlinear, uncertain, multiphysics and multiscale phenomenon. Brake squeal propensity is most often assessed through Complex Eigenvalue Analysis (CEA), yet many key parameters (e.g. friction, contact conditions, wear) are uncertain, time-varying and difficult to characterize. This makes surrogate models particularly attractive, as they aim to predict stability over a wide parameter space while limiting the number of high-fidelity simulations or tests. In this framework, one can distinguish (1) data that evolve with the contact interface (friction coefficient, surface topography, wear state, local temperature) and (2) data mainly linked to design and operating conditions (geometry, materials, loading). Properly capturing the nonlinear evolution and uncertainties of the first category, together with those of the second, is essential for reliable squeal prediction and robust stability assessment.

(1) Time-varying parameters such as friction coefficient or pad inclination can significantly affect contact stability. Surrogate modeling approaches using random sampling have been developed to explore this variability efficiently [1, 2].

(2) Uncertainties in material properties and geometry, including elastic modulus, damping or manufacturing tolerances, have also been shown to play a key role. Polynomial Chaos Expansion (PCE) methods have been used to model the stochastic response of brake systems under such uncertainties [3, 7].

(3) Hybrid models combining both sources of variability have been proposed more recently. Denimal et al. [4] developed a hybrid surrogate model based on Kriging and PCE to account simultaneously for evolving parameters and stochastic inputs, enabling robust squeal prediction with reduced computational cost.

Recent work by El Attaoui [5] and Lai [6] has demonstrated that the state of the contact surface plays a crucial role in the squeal triggering mechanism. Building on these studies, an experimental campaign was conducted, showing that specific contact localisations can significantly modify squeal propensity.

In line with this recent work, an uncertainty-aware numerical analysis is carried out : uncertainties in both the contact surface and the pin material, quantified experimentally, are propagated in a CEA to assess stability. Since a large amount of data is required to capture the nonlinear and transient nature of the phenomenon, a surrogate modelling strategy is implemented to identify the parameters that most strongly influence squeal propensity.

2 Statement of the experimental test of the friction test

An experimental friction campaign was carried out using a pin-on-disk test rig (Figure 1). The setup is equipped with dynamic sensors, including an eddy-current (Foucault) sensor used to measure the displacement of the load-carrying blade during braking, and a microphone to record the acoustic emission of the system. The surface topography of the pin is measured between successive braking tests in order to characterise the evolution of wear and the associated changes in contact conditions. In addition, the pin is instrumented with 12 embedded thermal sensors, which allow monitoring of the transient temperature field and, consequently, the evolution of the contact localisation during the braking tests.

The experimental campaign comprises 33 braking cycles, including an initial running-in phase consisting of 8 cycles. Each braking cycle is composed of 20 sequences, each consisting of 40 s of contact followed by 20 s without contact. An initial normal load of 200 N is applied, and the actual load is continuously monitored via the deflection of the blade. The rotational speed of the disk is maintained constant during a given cycle by adjusting the motor torque as needed. Constant-speed cycles (200, 400, and 600 rpm) are alternated with variable-speed cycles in order to assess the influence of the thermo-mechanical history on the dynamical response of the system.

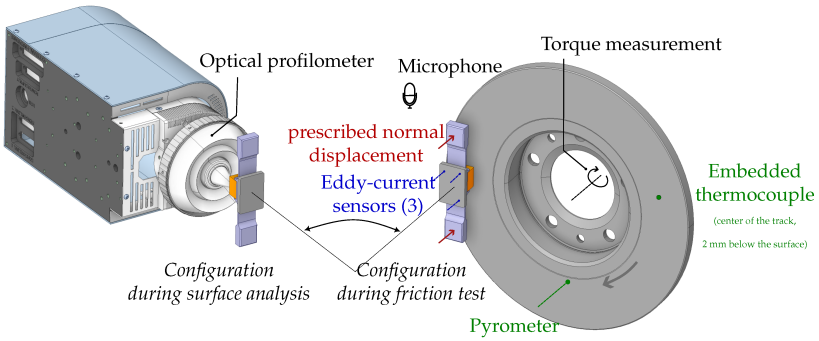

FIGURE 1 – Experimental pin-on-disk test setup with various sensors, showing a surface topography and the test configurations.

The system dynamics were characterised using a microphone that records acoustic emissions in the 0–50 kHz frequency range. A spectrogram of the microphone signal is computed over all experimental cycles (Figure 2) and post-processed to identify squeal occurrences and their corresponding frequencies. For clarity, the spectrogram in Figure 2 is truncated to the 2500–2950 Hz band, which contains a single instability. This instability is a fugitive squeal at approximately 2.8 kHz that appears only in cycles 15 and 24, both performed at 200 rpm, and is absent from other cycles conducted at the same speed (cycle 19 and cycle 28). All of these cycles were carried out under nominally identical braking conditions, with friction coefficients in the range 0.7–0.85 and temperatures during braking up to 70 °C.

To identify the triggering mechanism of this squeal, the evolution of the contact location was monitored using a multimodal sensor system (heat localisation, blade displacement, topography measurements, etc.). These measurements indicate that the 2.8 kHz squeal is associated with situations in which the contact area is well distributed over the four corners of the pin. Consequently, the occurrence of squeal at 200 rpm is not systematic but depends on the specific wear and thermo-mechanical history of the contact, which governs the surface state and its propensity to become unstable at 2.8 kHz.

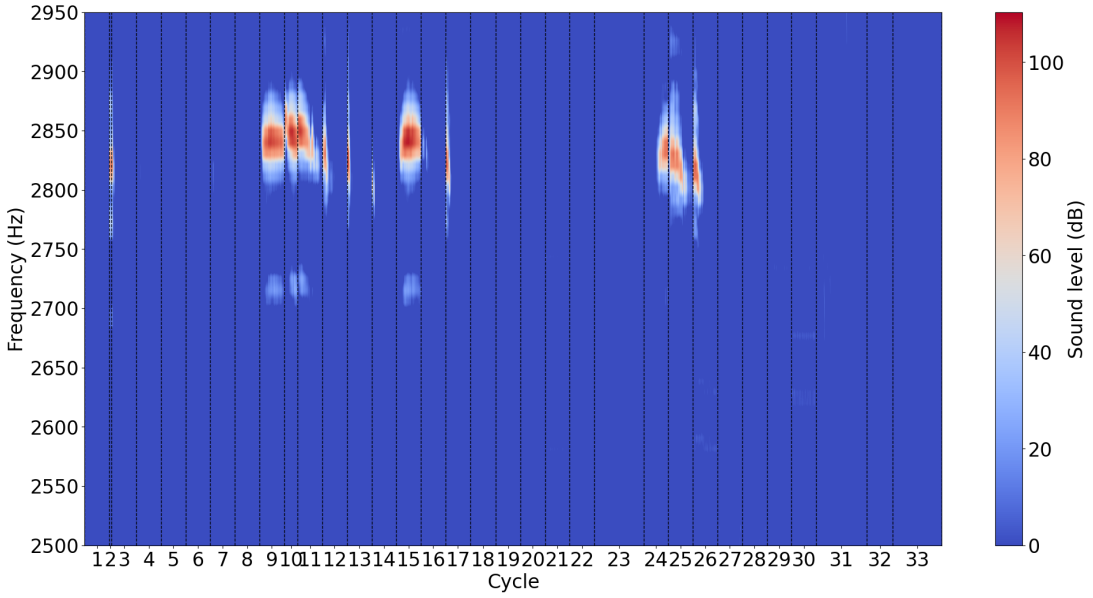

FIGURE 2 – Microphone spectrogram of acoustic emissions across test cycles

3 Numerical model

In this section, a parametric study is carried out in which the surface properties and material parameters are sampled within realistic bounds derived from the measurement dataset. The corresponding set of CEA simulations is used to train a multi-layer perceptron (MLP) surrogate model predicting the stability of the 2.8 kHz squeal associated with modal coupling. A sensitivity analysis of the MLP is then performed to identify the parameters that most strongly influence squeal propensity. The coupled modes obtained numerically are finally selected so that their operational deflection shapes match the experimentally measured one.

3.1 Quantification and modelling of uncertainties

A finite element model, together with its decoupled components, has been correlated with shock tests by minimizing both the Modal Assurance Criteria (MAC) error and the natural frequency error. Experimental observations show that the contact interface plays a key role in the triggering mechanism of instabilities. To account for this effect, the contact interface is modified by relocating the pin-side contact nodes, thereby changing the effective pin topography. Several parameters associated with the contact interface have been identified as influencing squeal propensity :

- **Tangential height difference θ position** : relative inclination of the pin in the sliding direction.
- **Form amplitude** : amplitude of the surface form obtained from topographic measurements between successive braking cycles.
- **Thermomechanical amplitude** : amplitude of the thermomechanical response of the pin.
- **Friction coefficient** : average value measured during the friction tests.
- **Radial height difference φ position** : relative inclination of the pin with respect to the disc in the radial direction.

Two additional parameters represent uncertainties associated with the braking material, identified from compression tests with digital image correlation :

- **Rayleigh damping coefficient** α : varied within a realistic range to assess its influence on stability, since direct experimental identification is difficult.
- **Young's modulus in the sliding direction** $\mathbf{E}_x$:, modelled as a normally distributed variable calibrated from compression tests ; the associated uncertainty arises from the measurement technique (digital image correlation). The braking material is assumed to be transversely anisotropic, with $\mathbf{E}_y$ taken as $\mathbf{E}_x - 300$.

The bounds used for the LHS sampling are described in Table 1.

TABLE 1 – Parameter bounds and probability distributions used in the simulations.

Variable	Min	Max	Probability distribution
Form amplitude	20 μm	50 μm	Uniform
Young's modulus E_x	1000 MPa	2200 MPa	Normal
Tangential height difference θ position	0 μm	100 μm	Uniform
Friction coefficient	0.4	0.85	Uniform
Thermomechanical amplitude	0 μm	100 μm	Uniform
Radial height difference φ position	-100 μm	100 μm	Uniform
Rayleigh damping coefficient α	100	500	Uniform

3.2 Definition of the database and modal classification

The objective of this section is to construct a surrogate model capable of predicting the real-valued quantity of interest associated with the 2.8 kHz mode, as a function of the contact-state variables and the material uncertainties. To this end, a dataset of 5000 simulations was generated by sampling the previously defined parameters using a Latin Hypercube Sampling (LHS) scheme. Each simulation was performed under an applied normal load of 200 N at the blade extremity, consistent with the experimental test. Since the modal basis evolves with the coupling interface, the surrogate model is built for a single coupled mode only. To this end, the modal bases in the dataset were classified using k-means clustering, and we retained the coupled mode around 2.8 kHz whose operational deflection shape of the blade matches the one identified from experimental data (Figure 3). After the classification step, 700 modes were retained.

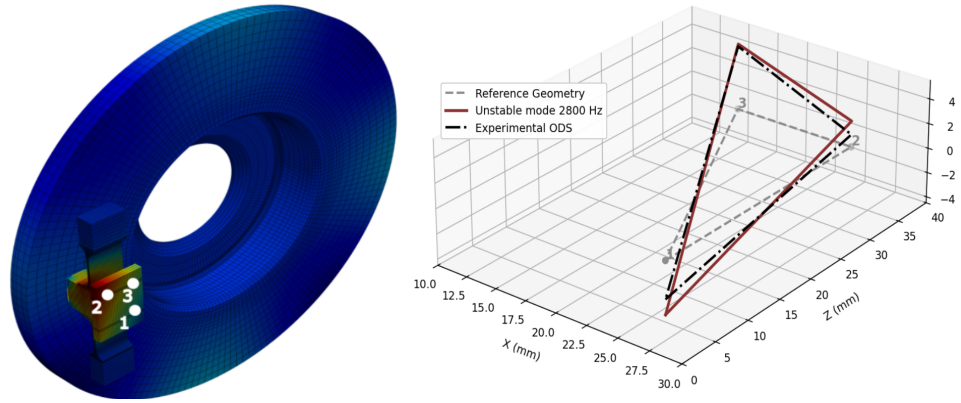

FIGURE 3 – Coupled mode unstable at 2.8 kHz from CEA analysis with the experimental Operational Deflection Shaped measured experimentaly

3.3 Surrogate modeling of stability

To develop the surrogate model, three approaches were compared : a MLP, polynomial chaos expansion (PCE), and Gaussian process regression (GP). All models were evaluated on a test set with 300 modes retained using three performance metrics : the root mean square error (RMSE), the rate of wrong stable (WP) (real value <0), and the rate of wrong unstable (WN) (real value >0).

The RMSE provides a global measure of the accuracy of the predicted real part of the eigenvalue over the whole test set. However, in practice, the sign and magnitude of this real part are directly related to the stability of the mode. For this reason, the WP and WN metrics are also introduced : WP quantifies the proportion of cases where the model incorrectly predicts an unstable behaviour, while WN quantifies the proportion of cases where an unstable mode is wrongly predicted as stable. These two complementary indicators are essential to assess the practical relevance of the surrogate model in terms of robustness.

For the three candidate models, hyperparameters were tuned on a validation set. The best performance, in terms of RMSE, WP and WN, was obtained with a MLP used as a regression model for the real part of the eigenvalue.

The MLP is chosen instead of the PCE and GP approaches because it provides a flexible nonlinear

mapping from the input features to the real part of the eigenvalue and scales well with the number of training samples and input dimensions. In particular, its capacity can be controlled through the network architecture and regularization hyperparameters, which allows us to balance approximation accuracy and robustness with respect to overfitting. All results reported in this section correspond to this final MLP trained on the full set of 700 retained modes.

The final MLP architecture consists of two fully connected hidden layers with 128 and 64 neurons, respectively, each followed by a ReLU activation. To mitigate overfitting, a dropout layer with a rate of 0.10 is applied after each hidden layer, together with an ℓ_2 weight decay of 10^{-4} on all trainable parameters and early stopping with a patience of 200 iterations on the validation loss. The network is trained with the AdamW optimizer using a fixed learning rate of 2×10^{-3} and a minibatch size of 128 samples. Both the input features and the target are standardized to zero mean and unit variance, which improves the conditioning of the optimization problem and stabilizes training. The main hyperparameters of this final MLP model are summarized in Table 2.

TABLE 2 – Main hyperparameters of the final MLP model trained on the full dataset

Hyperparameter	Value	Description
Hidden layer sizes	$(128, 64)$	Two fully connected hidden layers
Activation function	ReLU	Applied after each hidden layer
Dropout rate	0.10	Dropout applied after each hidden layer
Optimizer	AdamW	Adaptive optimizer with weight decay
Learning rate	2×10^{-3}	Fixed learning rate for AdamW
Weight decay	1×10^{-4}	ℓ_2 regularization strength
Batch size	128	Minibatch size for training
Early stopping patience	200	No-improvement iterations before stopping
Normalization	Standardization	Zero-mean, unit-variance for inputs and output

On the held-out test set, the selected MLP achieves a RMSE of 14.23 on the real part of the eigenvalue. In terms of stability assessment, the false-negative rate, i.e. the proportion of truly unstable modes that are incorrectly predicted as stable, is 6.54 %, whereas the false-positive rate, corresponding to truly stable modes wrongly predicted as unstable, is limited to 1.68 %. In the WP/WN notation introduced above, this corresponds to $WN = 6.54\,\%$ and $WP = 1.68\,\%$. These values indicate that misclassifications remain relatively uncommon and the model exhibits a good global regression accuracy on the real part of the eigenvalue as reflected by the RMSE.

3.4 Sensitivity analysis

The feature importance was quantified using the SHAP method (*SHapley Additive exPlanations*), which is based on Shapley values from cooperative game theory. For each prediction of the MLP, SHAP decomposes the output into additive contributions of each input variable ; by averaging the absolute value of these contributions over all samples, a global importance index is obtained for every parameter.

As shown in Figure 4, the form amplitude is by far the most influential parameter, followed by E_x and the tangential height difference θ position. The friction coefficient and the thermomechanical amplitude have a secondary but non-negligible impact, whereas the radial height difference φ position and the Rayleigh damping coefficient α contribute very little. These results highlight that surface and local contact-geometry parameters must be carefully considered to accurately model squeal instabilities, while realistic variations of global damping have a much smaller effect on the predicted stability.

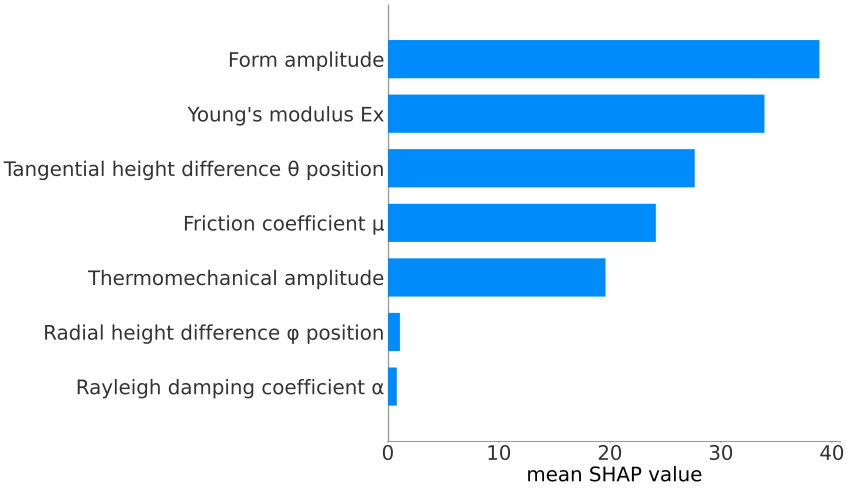

FIGURE 4 – Important feature obtained from MLP by shap method

To illustrate the influence of the interface parameters, one unstable sample from the LHS design is selected as a reference configuration, defined by Young's modulus $\mathbf{E}_x = 2168$ MPa, friction coefficient $= 0.731$, thermomechanical amplitude $= 6\,\mu$m, tangential height difference θ position $= 48\,\mu$m, Rayleigh damping coefficient $\alpha = 317$, Radial height difference φ position $= -35\,\mu$m.

Starting from this reference configuration, only the form amplitude is varied from [20 µm to 50 µm] in order to assess its impact on modal coupling. As shown in Figure 5, two modes approach each other and eventually coalesce as the form amplitude increases, which is accompanied by an increase in the real part of the eigenvalue and thus a strengthening of the instability.

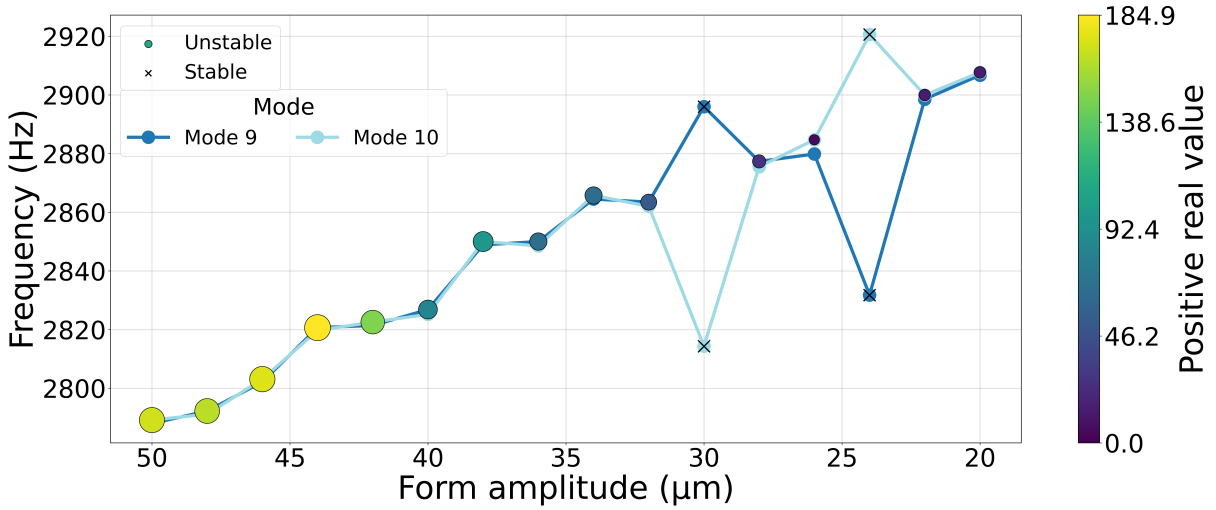

FIGURE 5 – Coalescence graph of the 2.8 kHz instability as a function of the form amplitude.

4 Conclusion

A dedicated surrogate modelling strategy has been developed to predict the 2.8 kHz squeal instability of a pin-on-disk system from contact-state variables and material uncertainties. Among the tested approaches, the multilayer perceptron offered the best trade-off between regression accuracy and reliable stability classification. The SHAP-based sensitivity analysis further revealed that surface-related parameters, in particular the form amplitude and tangential height difference θ position, are the dominant drivers of the instability, whereas realistic variations of damping and the radial height difference φ position misalignment have only a minor effect. These results highlight the crucial role of surface condition in the robust prediction of brake squeal. In addition, the strong influence of the pad material properties, especially the uncertainty on Young's modulus in sliding direction E_x, shows that material variability must also be explicitly accounted for to obtain reliable stability predictions.

Références

[1] E. Denimal, J.-J. Sinou, and S. Nacivet, Influence of structural modifications of automotive brake systems for squeal events with kriging meta-modelling method, *Journal of Sound and Vibration*, vol. 463, 2019, Art. no. 114938.

[2] A. Nobari, H. Ouyang, and P. Bannister, Uncertainty quantification of squeal instability via surrogate modelling, *Mechanical Systems and Signal Processing*, vol. 60–61, pp. 887–908, 2015.

[3] E. Sarrouy, O. Dessombz, and J.-J. Sinou, Piecewise polynomial chaos expansion with an application to brake squeal of a linear brake system, *Journal of Sound and Vibration*, vol. 332, no. 3, pp. 577–594, 2013.

[4] E. Denimal, J.-J. Sinou, and S. Nacivet, Prediction of squeal instabilities of a FEM automotive brake with uncertain structural and environmental parameters with a hybrid surrogate model, *Journal of Vibration and Acoustics*, vol. 144, no. 2, 2022, Art. no. 021006.

[5] Y. El Attaoui, Modélisation des surfaces réelles de contact et de leur évolution : Intégration dans les simulations de crissement, PhD thesis, Université Polytechnique Hauts de France, INSA Hauts-de-France, 2022.

[6] V.V. Lai et al., Multi-Scale Contact Localization and Dynamic Instability Related to Brake Squeal, *Lubricants*, 2020.

[7] J.-J. Sinou et al., Mode coupling instability in friction-induced vibrations and its dependency on system parameters including damping, *European Journal of Mechanics - A/Solids*, vol. 26, no. 1, pp. 106–123, 2007.